ChemPubSoc Europe

DOI: 10.1002/open.201402074

Open Access ChemistryOPEN Full Papers

Synthesis and Characterization of Layered Double Hydroxides and Their Potential as Nonviral Gene Delivery Vehicles

Blake Balcomb,[a] Moganavelli Singh,[b] and Sooboo Singh*[a]

Layered double hydroxides (LDHs) exhibit characteristic anion-exchange chemistry making them ideal carriers of negatively charged molecules like deoxyribonucleic acid (DNA). In this study, hydrotalcite (Mg–Al) and hydrotalcite-like compounds (Mg–Fe, Zn–Al, and Zn–Fe), also known as LDHs, were evaluated for their potential application as a carrier of DNA. LDHs were prepared by coprecipitation at low supersaturation and characterized by Powder X-ray diffraction (XRD), infrared (IR), Raman, and inductively coupled plasma—optical emission spectroscopy, scanning electron microscopy (SEM), and transmission electron microscopy (TEM). XRD patterns showed strong and sharp diffraction peaks for the (003) and (006) planes indicating well-ordered crystalline materials. TEM images yielded irregular circular to hexagonal-shaped particles of 50–250 nm in size. Varying degrees of DNA binding was observed for all the compounds, and nuclease digestion studies revealed that the LDHs afford some degree of protection to the bound DNA. Minimal toxicity was observed in human embryonic kidney (HEK293), cervical cancer (HeLa) and hepatocellular carcinoma (HepG2) cell lines with most showing a cell viability in excess of 80%. All LDH complexes promoted significant levels of luciferase gene expression, with the DNA:Mg–Al LDHs proving to be the most efficient in all cell lines.

Introduction

Although viral vectors are amongst the most efficient of all gene delivery vectors, majority of them suffer numerous draw backs such as the inability to produce high titers of the modified virus, elevated cytotoxicity, and activation of the immune response resulting from replication-competent viral particles. Nonviral vectors, on the other hand, such as liposomes, lipid nanoparticles, cationic polymers, organic and inorganic nanoparticles, as well as some biomaterials, exhibit lower immunogenic effects, simplicity, and feasibility of large-scale vector production. Many of these nonviral vectors, while exhibiting properties rendering them as attractive alternatives to viral vectors, have shown low gene delivery efficiency and transient gene expression. Despite this, researchers have persevered in the search, design, and synthesis of more favorable nonviral vectors. One such nonviral vector receiving much attention due to its favorable 'ideal' properties is the layered double hydroxide (LDH).

LDH compounds possess versatile properties such as good biocompatibility, low cytotoxicity, diverse functionality, controllable particle sizes, wide availability, high loading capacities, protection of biomolecules in the interlayers, and the potential for targeted delivery and controlled release of carried genes which make them appropriate for gene therapy. Of the various studies utilizing these compounds in gene therapy, most were carried out on Mg–Al since their structural and chemical properties have been extensively studied.[1a–e] LDHs are similar to the structure of brucite, $Mg(OH)_2$, in which each Mg^{2+} cation is octahedrally surrounded by six OH^- anions forming octahedral units which give rise to the layered sheeting arrangement of cations and anions. LDHs are represented by the formula $[M^{II}_{1-x}M^{III}_x(OH)_2]^{x+}$ $(A^{n-})_{x/y}\cdot yH_2O$, where M^{II} and M^{III} denote various possible divalent cations (Mg, Zn, Ni, Co, and Fe) and trivalent cations (Al, Fe, and Cr) respectively, and A^{n-} denotes interlayer exchangeable anions (CO_3^{2-}, Cl^-, and SO_4^{2-}).[2,3] It is these exchangeable anions that make LDHs excellent carriers of various anionic molecules. The stoichiometric ratio (x/y) may be altered to give varying types of LDH isostructural materials.[4,5] Traditionally, LDHs have been prepared by coprecipitation; however, other methods include hydrothermal treatments, separate nucleation and aging steps,[6] rehydration methods, and ion-exchange methods. Much attention has been focused on the ability of LDHs to store, remove, or carry anionic molecules by ion exchange. They have higher anion-exchange capacities than other anionic exchange resins and possess the added advantage of being readily synthesized in the laboratory from a variety of desired precursors.[7] Also, the chemical composition and structure of LDHs play an important role in their ion-

[a] B. Balcomb, Dr. S. Singh
School of Chemistry and Physics, University of KwaZulu-Natal
Private Bag X54001, Durban 4000 (South Africa)
E-mail: singhso@ukzn.ac.za

[b] Dr. M. Singh
School of Life Sciences (Biochemistry), University of KwaZulu-Natal
Private Bag X54001, Durban 4000 (South Africa)

exchange capacity A variety of inorganic and organic molecules has been intercalated and adsorbed by LDHs, such as oxoanions,[8a–c] deoxyribonucleic acid (DNA),[9] amino acids and oligopeptides,[10,11] and a number of pharmaceutical drugs.[12a–g]

The synthesis and study of LDHs have been going on for several decades. Apart from being used as catalysts, they are interesting for their potential use in electronics,[13a,b] drug or gene delivery,[14a–d] vaccinations,[15] and imaging.[16a,b] LDHs such as $Mg_6Al_2{\cdot}(OH)_{16}CO_3{\cdot}4H_2O$ have been and are to date being used as pharmaceutical antacids in the treatment of ulcers.[1e,17] Besides DNA, focus has been on the intercalation of siRNA into LDHs for gene therapy, for example silencing of the HT gene in Huntington's disease using RNA interference.[18] Furthermore, studies conducted by Li and co-workers showed that vaccination of syngeneic mice with an LDH:DNA complex induced the generation of antigen-specific cytotoxic T lymphocytes leading to antitumor effects.[15] More recently, fluorescein dye molecules have been incorporated into LDH nanoparticles to form nanocomposites or nanohybrids for the potential use in optical devices or biological applications.[16a] Most of the divalent and trivalent metal cations used to synthesize LDHs have low toxicity, and, hence, their potential use as drug or gene carriers and the use of MgAl–LDH–CO_3 as antacids attest to their low toxicity.

In this study, Mg–Al, Mg–Fe, Zn–Al, and Zn–Fe compounds were synthesized and characterized. Thereafter, their DNA binding, cytotoxicity, and transfection activities were investigated in vitro in three human cell lines, namely embryonic kidney (HEK293), cervical cancer (HeLa), and hepatocellular carcinoma (HepG2).

Results and Discussion

Characterization of the layered double hydroxides

Synthesized compounds Mg–Al and Zn–Al were white, whereas Mg–Fe and Zn–Fe were rust brown in color. The metal ratio for each compound is indicated in Table 1. The Mg:Al values showed a range of 0.26–0.34:1, in agreement with those reported in literature.[2] The Mg:Fe values showed a range of 0.6–0.8:1. There is a fairly equal distribution of both cations within the brucite-like layers, and this could be attributed to the fact that these cations have very similar ionic radii (Mg^{2+} = 0.65 Å, Fe^{3+} = 0.64 Å). Hence, it is possible that the two cations would position themselves fairly evenly throughout metal positions within the brucite-like layer. Zn–Al LDH samples, on the other hand, showed a greater amount of Zn with x being lower than calculated M^{II}:M^{III} values. Rojas Delgado et al.[19] reported that Zn–Al LDHs can be obtained with M^{II}:M^{III} values ranging from 1–5 due to electrostatic repulsion between trivalent metals. Also, they suggested that too high M^{II}:M^{III} values could result in a collapse of the interlayer region as they are less populated by charge-compensation anions. In this case, increase in the value of x is due to greater substitution of Zn^{2+} by Al^{3+} within the brucite-like layer, which increases the electrostatic attraction between the brucite-like layers and the interlayer anions. This attraction results in an observed compression of the LDH structure. In addition, increasing amounts of Al^{3+} within the brucite-layer results in greater repulsion of neighboring Al^{3+} ions.[20]

Powder X-ray diffraction (XRD) patterns of the different LDH compounds and Mg–Al:DNA are displayed in Figure 1 respectively. In general, XRD diffractograms for the compounds show sharp, symmetric, and intense lines at low 2θ values and less intense and generally asymmetric lines at higher 2θ values.[21] The sharp intense lines and a doublet peak at a 2θ value of 60° indicate the existence of an ordered layered material. Other diffraction peaks distinctive of an LDH structure are shown (marked with ● in Figure 1a) and correspond to Joint

Table 1. Elemental composition and XRD data for Mg–Al, Mg–Fe, Zn–Al, and Zn–Fe LDHs.

Compd	Elemental composition Calculated	Elemental composition Measured	Stoichiometry [x]	d_{003} basal spacing [Å]
	3:1	2.9:1	0.26	7.90
Mg–Al	2.3:1	2.2:1	0.31	7.77
	2:1	1.9:1	0.34	7.69
	3:1	0.8:1	0.55	7.85
Mg–Fe	2.3:1	0.7:1	0.58	7.84
	2:1	0.6:1	0.62	7.83
	8:1	8:1	0.11	7.69
Zn–Al	6:1	6.3:1	0.14	7.71
	5:1	5.4:1	0.16	7.69
	3:1	3.1:1	0.24	6.87
Zn–Fe	2.3:1	2.3:1	0.30	6.87
	2:1	2.1:1	0.32	6.89

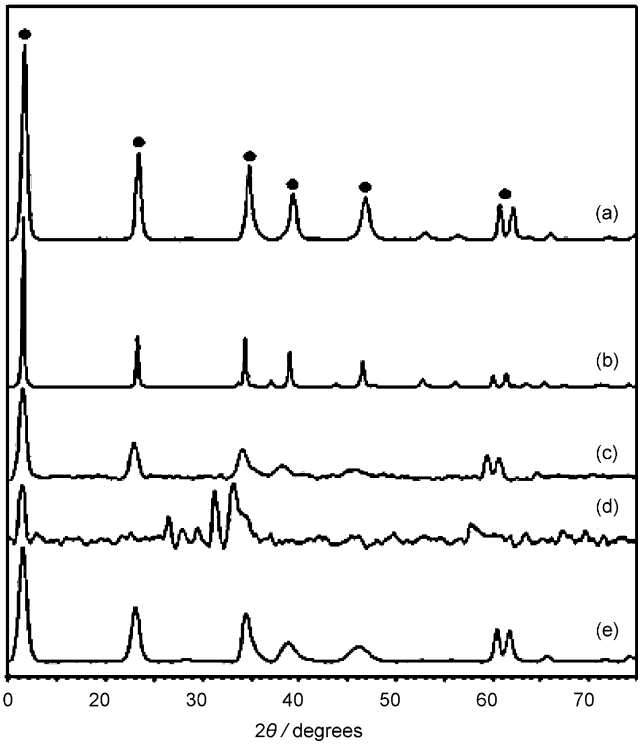

Figure 1. Powder XRD patterns of a) Mg–Al (● diffraction peaks distinctive of an LDH structure), b) Mg–Fe, c) Zn–Al, d) Zn–Fe, and e) Mg–Al:DNA.

Committee on Powder Diffraction Standards (JCPDS) File No. 22-700. The diffraction pattern of Zn–Fe shows an amorphous-type pattern, although characteristic LDH diffraction peaks are observed. This may in part be due to the small crystallite size of 1.6 nm (calculated from the Scherer equation) that perhaps is not fully resolved by the X-ray diffractometer.

The infrared (IR) spectra of Mg–Al and Mg–Al:DNA are shown in Figure 2. A broad peak at 3395–3450 cm^{-1} and a weak one at 1636–1367 cm^{-1} correlate to ν(OH) and δ(H_2O)

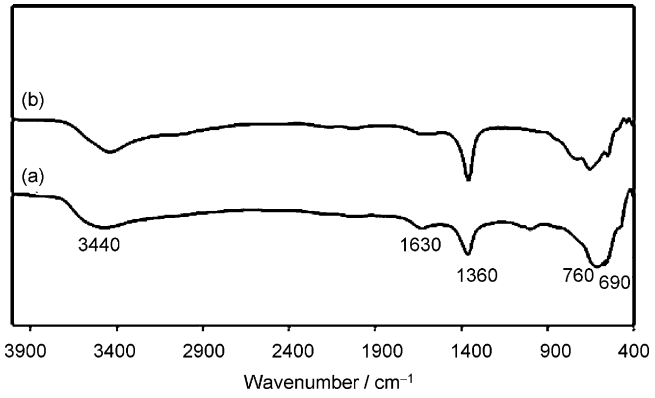

Figure 2. IR spectra of a) Mg–Al and b) Mg–Al:DNA.

bands respectively. Peaks at 650–665 cm^{-1} and 410–446 cm^{-1} are assigned to M–O vibrations and M–O–H bending, where M = Mg and Al. The sharp singlet observed at 1300–1362 cm^{-1} is due to the stretching of the carbonate ion.[2,3,22] According to Xu et al.[1c] and Valcheva–Traykova et al.,[23] sharp peaks at 446 cm^{-1} and 1352 cm^{-1}, doublet peaks at 769 cm^{-1} and 661 cm^{-1}, and a broad peak at 3396 cm^{-1} are all characteristic of an LDH structure. All the other compounds show similar features in their respective spectra.

The Raman spectra for Mg–Al samples exhibit strong broad bands at around 400–480 cm^{-1} which are associated with linkage oxygen bonds of brucite-like layer, metal–O–metal as well as metal–OH_2-coordinated water.[24] A weak band that appears at 800–830 cm^{-1} is due to the v_1 vibrational mode of CO_3^{2-} interacting with the hydroxyl groups of the brucite-like layer. A weaker band at around 1050 cm^{-1} could be attributed to the v_1 vibrational mode of CO_3^{2-}. A slightly stronger band is observed in the 2400 cm^{-1} due to weak v_1 vibrational modes of adsorbed CO_2 interacting weakly with the interlayer region.

Sonication in 95% ethanol for 30 min yielded an even distribution of particles when viewed under the TEM, compared to unsonicated samples which yielded denser aggregates of particles. All ratios of compounds yielded images that showed irregular circular to hexagonal shaped particles of 50–300 nm in diameter (Figure 3).

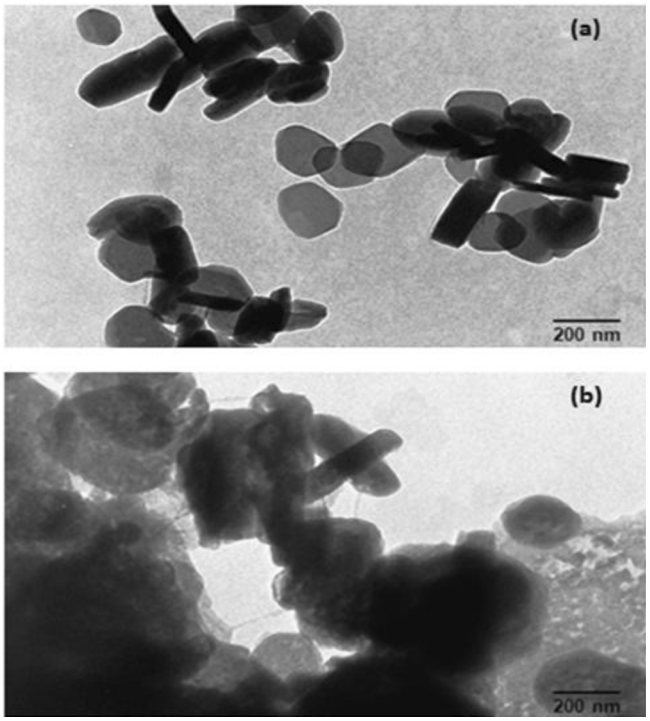

Figure 3. Representative TEM image of a) Mg–Al and b) Mg–Al:DNA.

Binding studies

From band-shift assays, all LDH samples showed the ability to electrostatically bind DNA at varying degrees (Figure 4a–d). LDHs exhibit an anion interlayer that is able to undergo ion exchange. Many researchers have exploited this property giving rise to a wide variety of applications such as the removal of toxic anions and herbicides from water and the ion exchange of various pharmaceuticals and biomolecules, including the intercalation of DNA.[25]

From Figure 4a, **MgAl.26** partially retarded the migration of DNA into the gel, that is, the compound was able to bind some of the DNA in solution. The unbound DNA in sample **MgAl.26** is thus able to migrate as free DNA and hence resembles the standard DNA (lane 1) with supercoiled (migrated furthest) and closed circular forms visible. Further increase in the ratio of DNA:**MgAl.26** (*w*/*w*) of up to 1:55 showed no further binding of DNA. **MgAl.31** and **MgAl.34** on the other hand, showed complete retardation at ratios 1:50 and 1:45 respectively.

All Zn–Al LDH samples (Figure 4b) showed very little binding of DNA with faint bands visible. Here again, any increase in weight ratios produced no change in the retardation pattern, and, hence, no change in their DNA-binding ability. Importantly, it is observed that the band of supercoiled DNA, that is, the band that migrates the furthest into the gel, was totally bound by the Zn–Al LDHs while the other forms of DNA were not. This is confirmed by the absence of the supercoiled band compared to the standard DNA (lane 1).

A similar pattern was seen for Zn–Fe LDH samples (Figure 4c), in which partial retardation was observed with higher ratios reflecting no further change in retardation pattern. Zn–Fe LDH samples also appeared to preferentially bind the supercoiled DNA, with the exception of **ZnFe.30** (Figure 4c, lanes 5, 6, 7) in which the band of supercoiled DNA is evident. Thus

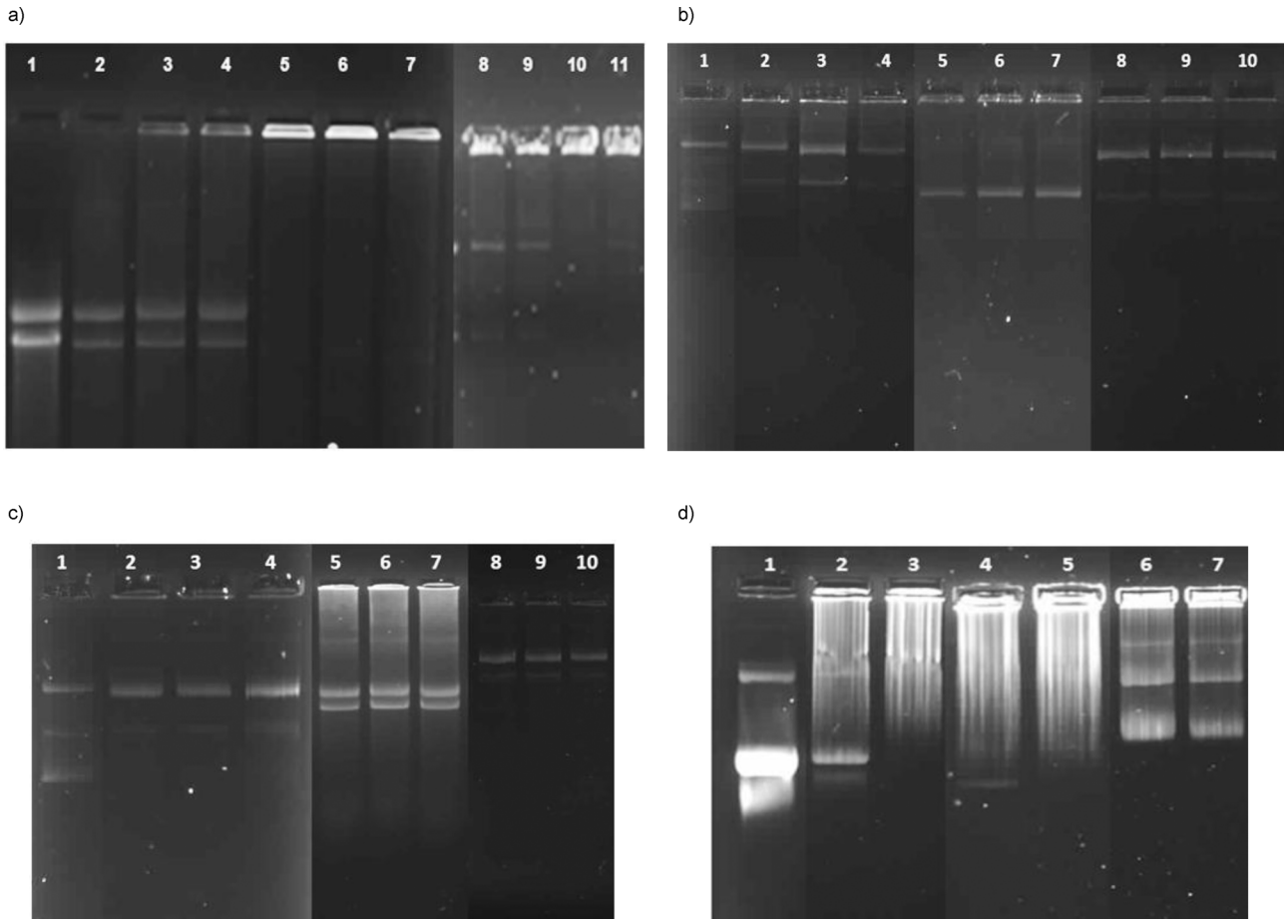

Figure 4. Band-shift assay of a) Mg–Al LDH. Lane 1: pCMV-Luc DNA (0.5 μg), lanes 2–4: pCMV-Luc:**MgAl.26** (1:35–1:45), lanes 5–7: pCMV-Luc:**MgAl.31** (1:50–1:60), lanes 8–11: pCMV-Luc:**MgAl.34** (1:30–1:45). b) Zn–Al LDH. Lane 1: pCMV-Luc DNA (0.5 μg), lanes 2–4: pCMV-Luc:**ZnAl.11** (1:60–1:70), lanes 5–7: pCMV-Luc:**ZnAl.14** (1:40–1:50), lanes 8–11: pCMV-Luc:**ZnAl.16** (1:40–1:50). c) Zn–Fe LDH. Lane 1: pCMV-Luc (0.5 μg), lanes 2–4: pCMV-Luc:**ZnFe.24** (1:30–1:40), lanes 5–7: pCMV-Luc:**ZnFe.30** (1:30–1:40), lanes 8–11: pCMV-Luc:**ZnFe.32** (1:30–1:40). d) Mg–Fe LDH. Lane 1: pCMV-Luc DNA (0.5 μg), lane 2: pCMV-Luc:**MgFe.55** (1:20), lane 3: pCMV-Luc:**MgFe.55** (1:30), lane 4: pCMV-Luc:**MgFe.58** (1:40), lane 5: pCMV-Luc:**MgFe.58** (1:50), lane 6: pCMV-Luc:**MgFe.62** (1:30), lane 7: pCMV-Luc:**MgFe.62** (1:40).

both Zn–Al and Zn–Fe LDHs appear to have a preference for the supercoiled DNA form.

MgFe.55 and **MgFe.58** (Figure 4d) showed complete retardation at about 1:30 (lane 3) and 1:50 (lane 5) respectively. **MgFe.62** showed partial retardation, with more bound DNA seen in the well than free DNA. The gel retardation pattern of **MgFe.62** was similar to that of Zn–Al and Zn–Fe samples. Thus, the ion-exchange conditions for these samples were reevaluated, and through time-dependent gel retardation, the optimum incubation time was determined as 72 h. Improved DNA retardation was obtained; however, streaking is observed throughout the gel, which could be attributed to DNA degradation due to prolonged incubation at 60 °C or the LDH itself.

At the point of complete retardation (as observed on the gels) where all the DNA was LDH-bound due to electrostatic interaction, the DNA:LDH complex is considered to be electroneutral. However, many of the DNA:LDH complexes underwent partial retardation suggesting that the DNA was unable to undergo complete ion exchange resulting in some of the DNA protruding out of a LDH particle. These were then able to electrostatically bind to the neighboring LDH particles in solution and hence form aggregates of DNA:LDH complexes. This was confirmed by XRD (Figure 1e) and IR spectroscopy (Figure 2b). From XRD patterns, no change in the XRD diffractogram or d-spacing values was observed. In addition, if DNA intercalated within the interlayer, a peak at a 2θ value of about 5–9° with a value of 23.7 Å should have been observed since the diameter of DNA is 23.7 Å.[26,27] However, from XRD software analysis, a peak showing an intensity of 1.0% was observed at a 2θ value of 6.3° with a d-spacing value of 14.01 Å. This is slightly larger than half the diameter of DNA which leads us to propose that perhaps the DNA binds to the outside of the LDH and is further compacted or sandwiched between one or more particles. If this is the case, due to the electrostatic interaction, one would observe no IR bonding frequencies between the LDH and the DNA; therefore, the IR spectrum should exhibit a mixture of the LDH and that of 'free' DNA. From the IR spectrum, there appears to be no bonding frequencies between the LDH and DNA and no evidence of 'free' DNA. The absence of free DNA in the IR spectrum could be due to the low amount of DNA in relation to the overwhelming amount of the LDH. Hence, IR bonding frequencies were not visible for

DNA or, simply, the intensity of these bonding frequencies was too low to overcome the background threshold.

Serum nuclease protection studies

From gel retardation assays for Mg–Al LDH samples, complete retardation was observed for DNA:**MgAl.31** and DNA:**MgAl.34** complexes. Nuclease protection assays performed on these complexes (Figure 5) showed little degradation of the DNA by the nucleases in the serum when compared to that of the naked/unbound DNA (lane 2) which was completely broken down.

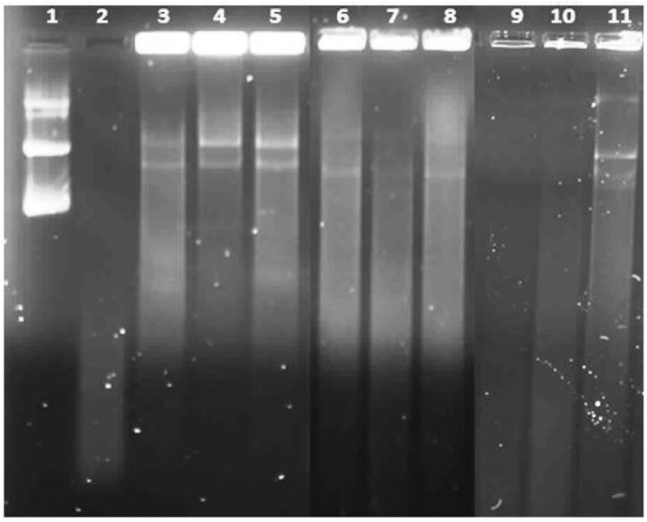

Figure 5. Nuclease digestion assay of **MgAl.26** LDH, **MgAl.31** LDH and **MgAl.34** LDH. Lane 1: pCMV-Luc (0.5 μg), lane 2: pCMV-Luc (0.5 μg) + 10% FCS, lane 3: **MgAl.26** (1:35), lane 4: **MgAl.26** (1:40), lane 5: **MgAl.26** (1:45), lane 6: **MgAl.31** (1:50), lane 7: **MgAl.31** (1:55), lane 8: **MgAl.31** (1:60), lane 9: **MgAl.34** (1:35), lane 10: **MgAl.34** (1:40), and lane 11: **MgAl.34** (1:45).

In addition, for all gels, most of the DNA that was complexed to the LDH samples appeared to remain in the wells and was not totally released upon addition of the detergent, sodium dodecyl sulfate (SDS). This can be seen by the lighter bands within the gel and the intense fluorescence observed in the wells. The partial degradation of DNA in the **MgAl.31** and **MgAl.34** samples provides further evidence that the DNA did not completely intercalate through ion exchange but was either bound to the periphery of the LDH exterior, or that incomplete ion exchange occurred where the DNA was partially intercalated, leaving protruding DNA. Any DNA found on the exterior of the LDH samples would be afforded little protection by the LDH and would be digested by the serum nucleases. Some DNA degradation was also observed for **MgAl.26**, which could be attributed to the fact that partial gel retardation was observed for this sample, and all unbound DNA together with any peripheral DNA on the LDH would hence be digested by the nucleases.

The subsequent release of DNA from the DNA:LDH complexes at the end of the nuclease digestion was carried out using SDS. This detergent has been used successfully to release DNA from most complexes with nonviral vectors. However with most of the DNA:LDH complexes, it was unable to completely liberate the DNA from the complex resulting in the DNA remaining in the well, bound to LDH samples. This could perhaps be due to the anionic nature of SDS as well its small size in relation to DNA which favored intercalation into the DNA:LDH complex, forming a tight complex resulting in partial release of DNA. Hydrochloric acid and nitric acid of varying concentration ranges (100 mM–1 M) were also used for DNA release. However, inconsistent results were obtained and, in most cases, inefficient release of DNA. The slow controlled release of biomolecules and pharmaceutics from LDHs has been reported extensively.[9, 12e, 28]

The Mg–Fe, Zn–Al and Zn–Fe complexes (gels not shown) also showed a similar trend to the Mg–Al complex (Figure 5), in that the complexes did only partially bind the DNA as seen in the binding studies, which could contribute to the presence of degraded DNA in nuclease protection assays. Again, partial degradation of the DNA was observed.

This degradation of DNA upon encountering serum could decrease the DNA delivery efficiency especially in an in vivo system, alluding to the need for further optimization of these complexes. Intercalation of the DNA within the layers of the LDH has been shown to provide sufficient protection to the nucleic acid as well as to ensure its controlled release.[14c] Furthermore, the toxicity levels of many drugs were significantly reduced after intercalation into either zinc or magnesium nanocomposites.[1b,29]

According to Costantino et al.,[30] the selectivity of anions within the interlayer of LDHs is as follows: $CO_2^{3-} > SO_4^{2-} \gg OH^- > F^- > Cl^- > Br^- > NO_3^- > ClO_4^-$. They also inferred that LDHs containing nitrate anions are the most suitable precursors for the uptake of biologically active species, and the high electrostatic affinity of CO_3^{2-} potentially hinders the ion exchange of DNA into the LDH interlayer region. This supports the evidence obtained from XRD, FTIR, as well as nuclease digestion assays that show the DNA does not fully intercalate within the interlayer region of the LDH.

Cytotoxicity studies

The cytotoxicity of the complexes was determined by the 3-(4,5-dimethylthiazol-2-yl)-5-(3-carboxymethoxyphenyl)-2-(4-sulfophenyl)-2H-tetrazolium (MTS) assay. Figure 6 shows the cytotoxicity levels obtained for all LDH complexes in the HEK293 cells only. A similar trend was seen in the HepG2 and HeLa cell lines (graphs not shown). All samples showed low levels of cytotoxicity to all cell lines with only a few exceptions where the cell viabilities dropped below 70%. This was only seen in the HepG2 cell line where at a concentration of 20 μg/10 μL, **MgAl.26**, **ZnAl.11**, and **ZnFe.24** produced cell viabilities of 54%, 54%, and 68% respectively. Also significant was the observed cell proliferation, producing cell viabilities over 100% especially for the Fe-containing samples. This could be due to the increased amount of intracellular Fe, which in turn increas-

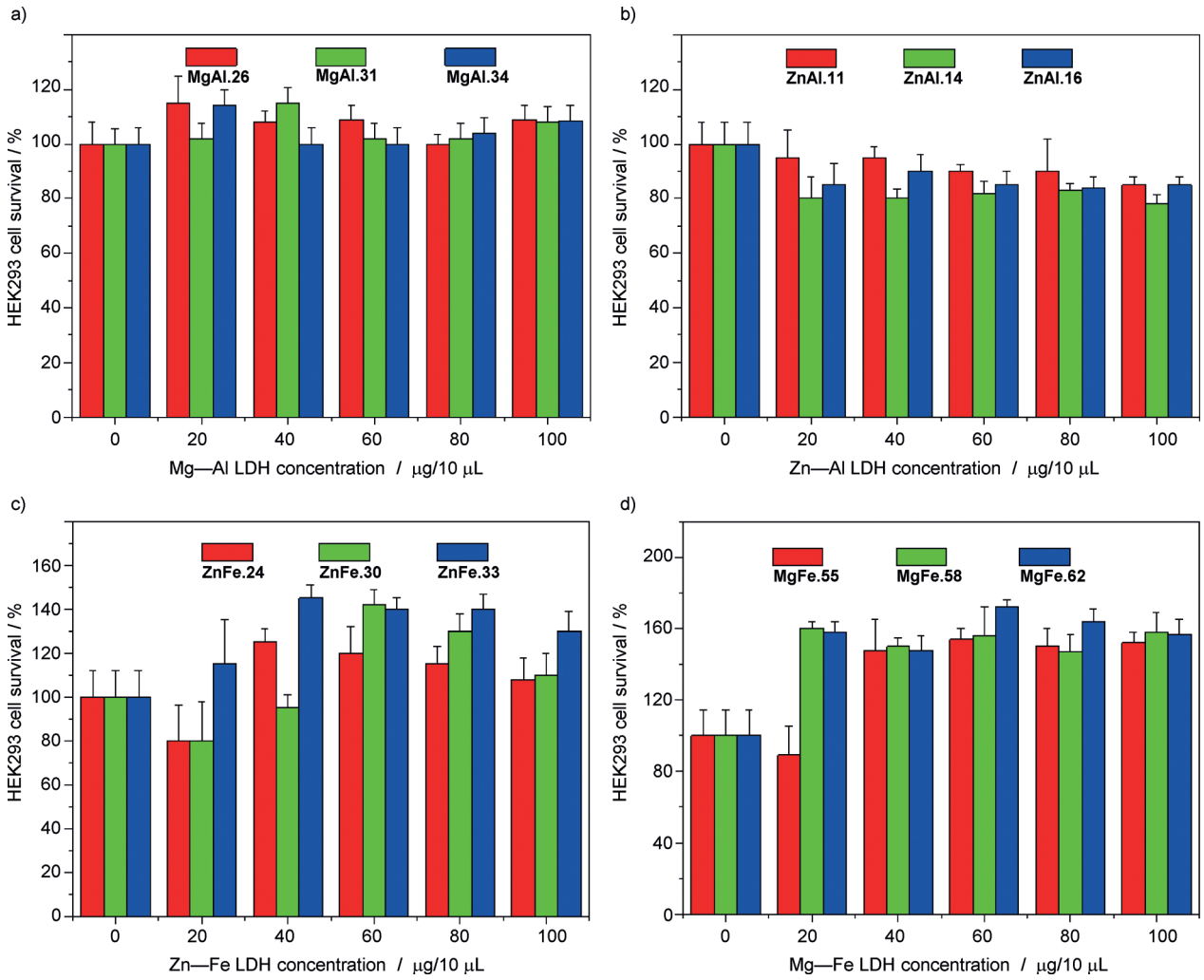

Figure 6. MTS cell proliferation assay of HEK293 cells exposed to a) Mg–Al LDH; b) Zn–Al LDH; c) Zn–Fe LDH; and d) Mg–Fe LDH. LDH concentration was varied (0, 20, 40, 60, 80, and 100 μg/10 μL). A control sample (0 μg/10 μL LDH) containing only HEK293 cells was assumed to have 100% survival. The assay was done in triplicate and data represent the mean ± S.D..

es the redox potential and the oxidative processes within the cells, producing higher cell viabilities.

In all cell lines it appears that the divalent cation may be responsible for variation in cell viabilities. Also the cell viabilities did not show any dose-dependent trend in all the cell lines. The low toxicity of Mg–Al LDHs seems to be consistent with literature.[12b,31] There appears to be no published data on the toxicity of Zn–Al, Zn–Fe, or Mg–Fe LDHs in literature. Due to their similar structures, chemistry, and binding studies that these LDHs exhibit to Mg–Al LDH, it is thus not surprising that there was little toxicity associated with these synthesized LDHs.

Furthermore, it can be noted that the levels of cell viability were also cell specific, with HEK293 and HeLa cells being more tolerant to the LDHs than the HepG2 cells. This cell-specific response may be attributed to differences in cellular uptake, cell surface characteristics, and intracellular trafficking and processing of the compounds in the three cell lines. This has been reported for other nonviral gene delivery vehicles.[32,33]

Transfection studies by luciferase reporter assays

The ability of these LDH:DNA complexes to successfully transfect the three human cell lines (HEK293, HeLa, and HepG2) in vitro with the pCMV-luc DNA reporter gene was determined using the luciferase reporter gene assay system (Promega). Generally all LDH:DNA complexes were able to produce transgene activity in the three human cell lines with the best transfection activity for all complexes observed in the HEK293 cells (Figure 7). This transfection activity was viewed against the two controls used (cells only and cells transfected with naked DNA) which showed negligible bioluminescence indicating little or no transfection of the reporter gene not complexed to the delivery vehicle. The highest transfection activity (16×10^4 RLU mg^{-1} protein) was observed for the DNA:**MgFe.55** (1:30 *w/w*) complex in the HEK293 cells (Figure 7d). This was almost twice the activity seen for the DNA:**ZnAl.11** (1:65 *w/w*) complex (Figure 7b) and eightfold greater than that obtained for the DNA:**MgAl.34** (1:35 *w/w*) and DNA:**ZnFe.24** (1:40 *w/w*)

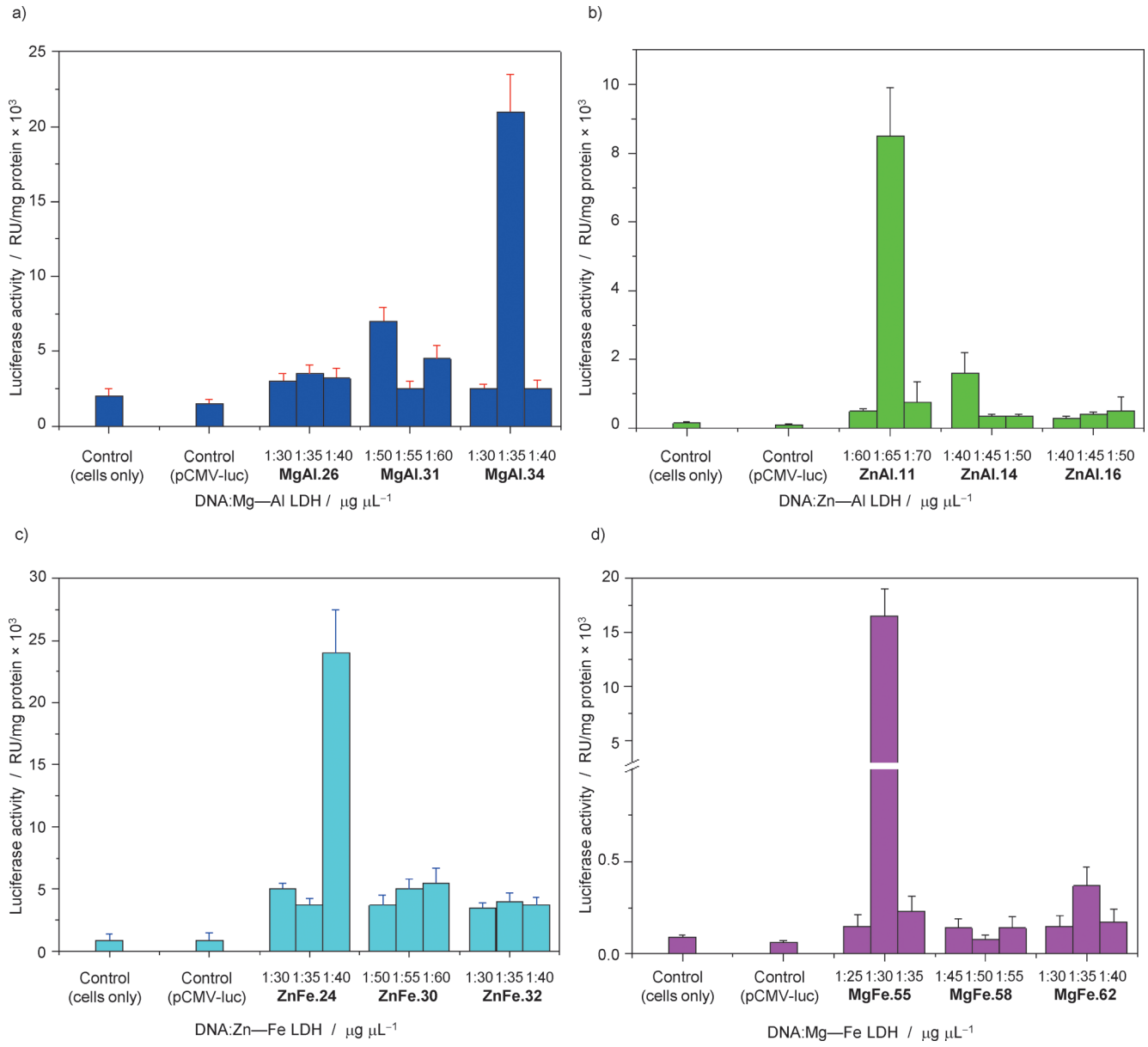

Figure 7. Luciferase activity in HEK293 cells using a) Mg–Al LDH, DNA: Mg–Al LDH (1:30–1:60); b) Zn–Al LDH, DNA:Zn–Al LDH (1:40–1:70), c) Zn–Fe LDH, DNA:Zn–Fe LDH (1:30–1:40); and d) Mg–Fe LDH, DNA:Mg–Fe LDH (1:25–1:55). The pCMV-luc DNA used was kept constant at 1.0 μg. Two controls were used: one containing only HEK293 cells and a second containing cells and pCMV-luc DNA (1.0 μg). The assay was conducted in triplicate, and data represent the mean ± S.D..

complexes (Figure 7 a, c). Overall the luciferase activities in the HepG2 and HeLa cells (results not shown) were much lower with no activity greater than 0.38×10^6 RLU mg^{-1} protein. The highest transgene activity in the HepG2 cells (0.38×10^6 RLU mg^{-1} protein) was for the DNA:**ZnAl.14** (1:40 *w/w*) complex, while the highest activity in the HeLa cells was obtained for the DNA:**MgAl.31**(1:60 *w/w*) complex. Overall, the DNA:Mg–Al LDHs produced best gene expression in the three cell lines.

Hence, there was no observed trend in relation to different ratios within an LDH composition group or between different groups. Although, it is thought that toxicity is directly related to efficient transfection in cells,[34] the high cell proliferation in the MTS assay seen for some samples (mostly Fe containing), however, did not necessarily translate into higher luciferase activities, especially in the HepG2 and HeLa cell lines. However, it is also interesting to note that the cell-specific cytotoxicity seems to correlate with a cell-specific transgene activity. When comparing transfection activities in different cell lines it is important to note that differences of complex internalization, endosomal escape, and processing of DNA into the nucleus can be cell specific. Also, these complexes did not release the DNA easily, as seen in the nuclease protection assay (Figure 5), which could also be a determining factor during endosomal release of the DNA in the cell. Furthermore, the sizes of the complexes ranged from 50–300 nm which could also affect the ability of the complexes to enter specific cell types. It has been suggested that complex sizes of 150 nm or less favor the pro-

cess of endocytosis,[35] and that large aggregates do not interfere with transfection. Since they cannot enter the cells by endocytosis, other cell entry mechanisms may be in place for the uptake of these larger complexes.[36]

Overall the luciferase activities in all three cell lines using DNA:LDH samples were promising. Hence, these LDHs have demonstrated the ability to efficiently bind and deliver DNA into selected mammalian cells in culture.

Conclusions

All LDH compounds exhibited the ability to bind DNA to varying degrees, which was further confirmed by XRD, FTIR, Raman spectroscopy, and electron microscopy. These compounds were further able to afford protection, partial in some cases, to the DNA cargo in the presence of serum nucleases. The results from the MTS cell proliferation assay showed that all complexes were well tolerated by the cells with most cell viabilities in excess of 70%. Significant luciferase transgene activity was observed for specific compounds which should be optimized in future studies. The results from this investigation show that some of the LDH compounds synthesized have the potential to be viable and interesting alternatives to other nonviral gene delivery systems.

Experimental Section

Reagents. The following reagents were obtained from Merck (Darmstadt, Germany): $Mg(NO_3)_2{\cdot}6H_2O$, $Al(NO_3)_3{\cdot}9H_2O$, $Zn(NO_3)_2{\cdot}6H_2O$, $Fe(NO_{3)3}{\cdot}9H_2O$, Na_2CO_3, NaOH, glycerol, bromophenol blue, xylene cyanol, ethidium bromide, Na_3PO_4, Tris-HCl, EDTA, SDS. The pCMV-Luc DNA plasmid was from The Plasmid Factory (Bielefeld, Germany), and the fetal calf serum (FCS) was from Gibco, Invitrogen (Paisley, UK). The MTS (CellTiter 96 Aqueous One Solution) cell proliferation assay and luciferase assay were from Promega (Madison, USA).

Preparation of layered double hydroxides. Four sets of compounds, 1) Mg^{2+}–Al^{3+}–CO_3^{2-}, 2)Mg^{2+}–Fe^{3+}–CO_3^{2-}, 3) Zn^{2+}–Al^{3}–CO_3^{2-}, and 4) Zn^{2+}–Fe^{3+}–CO_3^{2-} were prepared by coprecipitation at low supersaturation. In a typical preparation method involving Mg–Al LDH, a mixed aqueous solution of $Mg(NO_3)_2{\cdot}6H_2O$ (0.15 mol) and $Al(NO_3)_2.9H_2O$ (0.05 mol) was added dropwise to Na_2CO_3 (0.5 mol) solution. The pH was maintained at 11 ± 0.5 using NaOH, and the mixture was stirred vigorously throughout the addition of the metal solution. The resultant slurry was heated and maintained at 80°C for 18 h, filtered, washed, and finally dried in an oven set at 110°C for 12 h. A similar procedure was followed for the synthesis of the other compounds.

Characterization techniques. Powder XRD patterns were recorded on a D8 Advance X-Ray Diffractometer (Bruker, AXS GmbH, Germany). FTIR spectra were obtained using a Universal ATR spectrometer (PerkinElmer, Waltham, USA). Elemental composition was determined using an Optima 5300 DV Inductively Coupled Plasma–Optical Emission Spectrometer (ICP–OES) (PerkinElmer, Waltham, USA). For transmission electron microscopy (TEM), a small amount of each compound was suspended in 95% ethanol and sonicated. Thereafter, the suspension (1 μL) was fixed onto a copper grid. TEM images were captured on a 1010 Megaview 3 Soft Imaging TEM System (Jeol, Tokyo, Japan). Scanning electron microscopy (SEM) was performed on a Leo 1450 SEM (Leo Electron Microscopy Ltd., Jena, Germany). SEM–Energy Dispersive X-Ray Spectrometry was performed on a JSM6100 SEM (Jeol, Tokyo, Japan).

Binding studies. Association of LDH with plasmid DNA was demonstrated using the band-shift assay. Plasmid pCMV-Luc DNA was kept constant in all complexes at 0.5 μg while the amounts of LDH were varied (Figure 4). Samples were incubated at 60°C for 120 min. Thereafter, 2 μL gel loading buffer (50% glycerol, 0.05% bromophenol blue, 0.05% xylene cyanol) was added to each sample, which was loaded onto an eight-well 1% agarose gel containing 1.5 $\mu g\,mL^{-1}$ EtBr and run at 50 V for 120 min in electrophoresis buffer (36 mM Tris-HCl, 30 mM Na_3PO_4, 10 mM EDTA , pH 7.5). After electrophoresis, the gel was viewed and photographed under 300 nm UV transillumination in a Vacutec Syngene G-box gel documentation system (Syngene, Cambridge, UK).

Nuclease protection studies. Reaction complexes were prepared as for binding studies, using the optimum ratio, one ratio above, and one below (Figure 5). After incubation of the complexes, FCS was added to all samples to a final concentration of 10% (*v*/*v*) with a further incubation at 37°C for 4 h. Thereafter, EDTA and SDS were added to a final concentration of 10 mM and 0.5% (*w*/*v*) respectively. The complexes were incubated at 55°C for 20 min and then subjected to 1% agarose gel electrophoresis as above.

Cytotoxicity studies. The cytotoxicity of the LDH:DNA complexes was determined using the MTS (CellTiter 96 Aqueous One Solution, Promega) cell proliferation assay. The cells (HEK293, HepG2, HeLa) were trypsinized and seeded into respective 48-well plates at a density of 3.5×10^5 cells/well. Cells were incubated at 37°C for 24 h to allow them to attach to the wells and grow towards semiconfluency. LDH:DNA complexes were prepared at various ratios (Figure 6a–d). The cells were prepared by replacing the growth medium with 0.3 mL of fresh medium (Eagle's minimum essential medium (EMEM) + 10% FBS + 100 units penicillin G + 100 μg streptomycin sulphate/mL). The reaction complexes were then added to the cells followed by incubation of the cells at 37°C for 48 h. Assays were carried out in triplicate. Thereafter, the MTS reagent (40 μL) was added to each well, and cells incubated at 37°C for a further 4 h. Absorbance values were then recorded at 490 nm using a Biomate 3 spectrophotometer (Thermo Scientific, Waltham, USA).

Transfection studies. Cells were trypsinized and seeded into respective 48-well plates at a density of about 3.5×10^5 cells/well and incubated at 37°C overnight. DNA:LDH complexes were prepared as for protection studies, with the DNA constant at 1.0 μg. Complexes were then added to cells that were replenished with fresh medium (EMEM + 10% FBS + 100 units penicillin G + 100 μg streptomycin sulphate/mL), and cells were incubated at 37°C for 48 h. Two controls were used, cells only and cells with pCMV-luc DNA (1.0 μg). Briefly, following the 48 h incubation, the medium was removed, and cells were washed with phosphate buffered saline, (0.2 mL, pH 7.4), lysed with 80 μL of cell lysis reagent, and rocked for 15 min at 30 rpm. Cells were scraped from the wells, and cell suspensions centrifuged for 30 s at 12000 rpm to pellet cellular debris. The cell supernatants were then assayed for firefly luciferase activity according to the Promega Luciferase Assay protocol (Promega, Madison, USA).The luminescence obtained as relative light units were normalized against the protein content in the cell lysates using the bicinchoninic acid (BCA) protein assay (Sigma–Aldrich, St. Louis, USA). Readings were then were expressed as RLU/mg protein. The assay was conducted in triplicate.

Acknowledgements

The authors are grateful to the National Research Foundation of South Africa and University of KwaZulu-Natal for financial support during this study.

Keywords: DNA · gel retardation · gene delivery · layered double hydroxides · transfection vectors

[1] a) J. H. Choy, S. Y. Kwak, Y. J. Jeong, J. S. Park, *Angew. Chem. Int. Ed.* **2000**, *39*, 4041 – 4045; *Angew. Chem.* **2000**, *112*, 4207 – 4211; b) Z. P. Xu, G. Q. Lu, *Pure Appl. Chem.* **2006**, *78*, 1771 – 1779; c) Z. P. Xu, Q. H. Zeng, G. Q. Lu, A. B. Yu, *Chem. Eng. Sci.* **2006**, *61*, 1027 – 1040; d) Z. P. Xu, T. L. Walker, K.-l. Liu, H. M. Cooper, G. Q. H. Lu, P. F. Bartlett, *Int. J. Nanomed.* **2007**, *2*, 163 – 174; e) Z. P. Xu, M. Niebert, K. Porazik, T. L. Walker, H. M. Cooper, A. P. J. Middelberg, P. P. Gray, P. P. Bartlett, G. Q. H. Lu, *J. Controlled Release* **2008**, *130*, 86 – 94.

[2] F. Cavani, F. Trifiró, A. Vaccari, *Catal. Today* **1991**, *11*, 173 – 301.

[3] a) F. J. Brücker, L. Kainer, German Patent 2024282, **1970**; b) F. J. Brücker, L. Kainer, UK Patent 1342020, **1971**.

[4] B. Li, J. He, D. G. Evans, X. Duan, *Appl. Clay Sci.* **2004**, *27*, 199 – 207.

[5] N. Du, W. G. Hou, S. E. Song, *J. Phys. Chem. B* **2007**, *111*, 13909 – 13913.

[6] G. Evans, X. Duan, *Chem. Commun.* **2006**, 485 – 496.

[7] M. Islam, R. Patel, *Organic – Inorganic Hybrid Ion Exchangers and Layered Double Hydroxides: Synthesis, Characterization and Environmental Application*. Lambert Academic Publishing GmbH & Co. KG, Saarbrücken, Germany, **2009**.

[8] a) G. Mao, M. Tsuji, Y. Tamaura, *Clays Clay Miner.* **1993**, *41*, 731 – 737; b) E. Suzuki, S. Idemura, Y. Ono, *Clays Clay Miner.* **1989**, *37*, 173 – 178; c) C. Misra, A. J. Perrotta, *Clays Clay Miner.* **1992**, *40*, 145 – 150.

[9] H. Nakayama, A. Hatekeyama, M. Tsuhako, *Int. J. Pharm.* **2010**, *393*, 105 – 112.

[10] S. Aisawa, S. Sasaki, S. Takahashi, H. Hirahara, H. Nakayama, E. Narita, *J. Phys. Chem. Solids* **2006**, *67*, 920 – 925.

[11] Á. Fudala, I. Pálinkó, I. Kiricsi, *Inorg. Chem.* **1999**, *38*, 4653 – 4658.

[12] a) V. Ambrogi, L. Perioli, V. Ciarnelli, M. Nocchetti, C. Rossi, *Eur. J. Pharm. Biopharm.* **2009**, *73*, 285 – 291; b) Z. Gu, B. Rolfe, Z.-P. Xu, A. C. Thomas, J. Campbell, G. Q. M. Lu, *Biomaterials* **2010**, *31*, 5455 – 5462; c) S. Aisawa, N. Higashiyama, S. Takahashi, H. Hirahara, D. Ikematsu, H. Kondo, H. Nakayama, E. Narita, *Appl. Clay Sci.* **2007**, *35*, 146 – 154; d) M. del Arco, A. Fernández, C. Martín, V. Rives, *Appl. Clay Sci.* **2007**, *36*, 133 – 140; e) L. Qin, M. Xue, W. Wang, R. Zhu, S. Wang, J. Sun, R. Zhang, X. Sun, *Int. J. Pharm.* **2010**, *388*, 223 – 230; f) S. Carlino, M. J. Hudson, S. W. Husain, J. A. Knowles, *Solid State Ionics* **1996**, *84*, 117 – 129; g) M. Trikeriotis, D. F. Ghanotakis, *Int. J. Pharm.* **2007**, *332*, 176 – 184.

[13] a) K. Itaya, H. C. Chang, I. Uchida, *Inorg. Chem.* **1987**, *26*, 624; b) J. B. Qiu, G. J. Villemure, *Electroanal. Chem.* **1997**, *428*, 165.

[14] a) C. R. Gordijo, C. A. S. Barbosa, A. M. D. Ferreira, V. R. L. Contantino, D. D. O. Silva, *J. Pharm. Sci.* **2005**, *94*, 1135; b) J.-M. Oh, S.-J. Choi, G.-E. Lee, J.-E. Kim, J.-H. Choy, *Chem. Asian J.* **2009**, *4*, 67 – 73; c) S. Y. Kwak, Y.-J. Jeong, J.-S. Park, J. H. Choy, *Solid State Ionics* **2002**, *151*, 229 – 234; d) A. U. Kura, M. Z. Hussein, S. Fakurazi, P. Arulselvan, *Chem. Cent. J.* **2014**, *8*, 47.

[15] A. Li, L. Qin, W. Wang, R. Zhu, Y. Yu, H. Liu, S. Wang, *Biomaterials* **2011**, *32*, 469 – 477.

[16] a) L. Yan, Y. Wang, J. Li, S. Kalytchuk, A. S. Susha, S. V. Kershaw, F. Yan, A. L. Rogach, X. Chen, *J. Mater. Chem. C* **2014**, *2*, 4490 – 4494; b) P.-R. Wei, S.-H. Cheng, W.-N. Liao, K.-C. Kao, C.-F. Weng, C.-H. Lee, *J. Mater. Chem.* **2012**, *22*, 5503 – 5513.

[17] S. M. Beekman, *J. Pharm. Assoc.* **1960**, *49*, 191 – 200.

[18] H. Zhang, D. Ouyang, V. Murthy, Y. Wong, Z. Xu, S. C. Smith, *Pharmaceuticals* **2012**, *4*, 296 – 313.

[19] R. Rojas Delgado, C. P. De Pauli, C. Barriga Carrasco, M. J. Avena, *Appl. Clay Sci.* **2008**, *40*, 27 – 37.

[20] F. Thevenot, R. Szymanski, P. Chaumette, *Clays Clay Miner.* **1989**, *37*, 396 – 402.

[21] E. López-Salinas, M. García-Sánchez, J. A. Montoya, D. R. Acosta, J. A. Abasolo, I. Schifter, *Langmuir* **1997**, *13*, 4748 – 4753.

[22] S. Miyata, *Clays Clay Miner.* **1975**, *23*, 369 – 375.

[23] M. L. Valcheva-Traykova, N. P. Davidov, A. H. Weiss, *J. Mater. Sci.* **1993**, *28*, 2157 – 2162.

[24] H. S. Panda, R. Srivastava, D. Bahadur, *Mater. Res. Bull.* **2008**, *43*, 1448 – 1455.

[25] N. Morel-Desrosiers, J. Pisson, Y. Israël, C. Taviot-Guého, J. P. Besse, J.-P. Morel, *J. Mater. Chem.* **2003**, *13*, 2582 – 2585.

[26] K. Ladewig, M. Niebert, Z. P. Xu, P. P. Gray, G. Q. M. Lu, *Biomaterials* **2010**, *31*, 1821 – 1829.

[27] J. M. Berg, J. L. Tymoczko, L. Stryer, *Biochemistry, 6th ed.*, W. H. Freeman and Company, New York, **2006**.

[28] K. M. Tyner, M. S. Roberson, K. A. Berghorn, L. Lib, R. F. Gilmour Jr., C. A. Batt, E. P. Giannelis, *J. Controlled Release* **2004**, *100*, 399 – 409.

[29] K. Sugano, M. Kansy, P. Artursson, A. Avdeef, S. Bendels, L. Di, G. F. Ecker, B. Faller, H. Fischer, G. Gerebtzoff, H. Lennernaes, F. Senner, *Nat. Rev. Drug Discovery* **2010**, *9*, 597 – 614.

[30] U. Costantino, V. Ambrogi, M. Nocchetti, L. Perioli, *Microporous Mesoporous Mater.* **2008**, *107*, 149 – 160.

[31] Y. Wong, K. Markham, Z. P. Xu, M. Chen, G. Q. M. Lu, P. F. Bartlett, H. M. Cooper, *Biomaterials* **2010**, *31*, 8770 – 8779.

[32] H. Lv, S. Zhang, B. Wang, S. Cui, J. Yan, *J. Controlled Release* **2006**, *114*, 100 – 109.

[33] K. Romøren, B. J. Thu, N. C. Bols, O. Evensen, *Biochim. Biophys. Acta Biomembr.* **2004**, *1663*, 127 – 134.

[34] C. M. Wiethoff, C. R. Middaugh, *J. Pharm. Sci.* **2003**, *92*, 203 – 217.

[35] W. F. Bertling, M. Gareis, V. Paspaleeva, A. Zimmer, J. Kreuter, E. Nürnberg, P. Harrer, *Biotechnol. Appl. Biochem.* **1991**, *13*, 390 – 405.

[36] D. D. Lasic, *Liposomes in Gene Delivery*, CRC Press, Boca Raton, New York, **1997**.

Received: September 26, 2014
Published online on December 18, 2014

